

## **Interlocking cast glass components, Exploring a demountable dry-assembly structural glass system**

Oikonomopoulou, Faidra; Bristogianni, Telesilla; Barou, Lida; Jacobs, Erwin; Frigo, Giulia; Veer, Fred; Nijssse, Rob

**Publication date**

2018

**Document Version**

Final published version

**Published in**

Heron

**Citation (APA)**

Oikonomopoulou, F., Bristogianni, T., Barou, L., Jacobs, E., Frigo, G., Veer, F., & Nijssse, R. (2018). Interlocking cast glass components, Exploring a demountable dry-assembly structural glass system. *Heron*, 63(1/2), 103-138.

**Important note**

To cite this publication, please use the final published version (if applicable). Please check the document version above.

**Copyright**

Other than for strictly personal use, it is not permitted to download, forward or distribute the text or part of it, without the consent of the author(s) and/or copyright holder(s), unless the work is under an open content license such as Creative Commons.

**Takedown policy**

Please contact us and provide details if you believe this document breaches copyrights. We will remove access to the work immediately and investigate your claim.

# Interlocking cast glass components, Exploring a demountable dry-assembly structural glass system

Faidra Oikonomopoulou <sup>a</sup>, Telesilla Bristogianni <sup>a</sup>, Lida Barou <sup>a</sup>, Erwin Jacobs <sup>a</sup>, Giulia Frigo <sup>b</sup>, Frederic A. Veer <sup>a</sup>, Rob Nijse <sup>a</sup>

<sup>a</sup> Delft University of Technology, the Netherlands, f.oikonomopoulou@tudelft.nl

<sup>b</sup> Politecnico di Milano, Italy

This paper explores the potential of a novel, reversible all-glass system consisting of dry-assembly, interlocking cast glass components. Owing to its interlocking geometry, the proposed system can attain the desired stiffness with the aid of minimal, if any, metal framing. The use of adhesives is circumvented in the system by employing a dry, colourless interlayer as an intermediate medium between the glass components. The interlayer can accommodate by deformation surface asperities; furthermore, it allows for an even stress distribution and for the eventual disassembly and reuse of the components. To validate the concept, various component geometries and interlocking mechanisms are developed. The interlocking forms are kiln cast in 1 : 2 scale and are comparatively assessed in terms of mechanical interlocking capacity, mass distribution, residual stress generation and ease of fabrication. In parallel, research is conducted on different materials for the dry, transparent interlayer. From the developed designs, osteomorphic blocks are selected as the most promising concept and are further assessed by numerical modelling to investigate the influence of the interlocking geometry to the overall structural performance. The results of the numerical model indicate that lower bricks are more susceptible to bending, whereas for higher brick variants the shear lock failure is more critical. To further validate the concept, two specimens of stacked glass columns comprising osteomorphic blocks and different interlayers are tested in compression until failure. The failure mode of the specimens suggests an increased fracture toughness of the proposed system compared to a monolithic variant, preventing cracks propagating from one brick to another and an inherent robustness. The experiments also suggest that an interlayer of increased shear strength is recommended to prevent tearing under compression and thus avoiding direct glass-to-glass contact.

*Keywords: Cast glass, interlocking geometry, interlocking components, dry-assembly, glass structures, reversibility, glass connections, structural fragmentation*

# 1 Introduction

Solid cast glass components are a promising solution for engineering pure glass structures of high transparency and load-carrying capacity; a solution that so far has been little explored in architecture. At present, only a few realized examples of self-supporting structures out of solid cast glass elements exist<sup>1</sup> (fig. 1). The most characteristic ones are the envelopes of the *Atocha Memorial* (Schober et al. 2007), the *Crown Fountain* (Hannah 2009), the *Optical House* (Hiroshi 2013) and the *Crystal Houses* (Oikonomopoulou et al. 2015b). To ensure the desired stiffness of the glass assembly, these projects rely either on a metal substructure or on a rigid, colourless structural adhesive, less than 2 mm thick, (Goppert et al. 2008; Oikonomopoulou et al. 2015b) to bond the blocks together. Whereas the solution of an additional substructure compromises the overall level of transparency, the solution of a rigid adhesive leads to a permanent construction of intensive and meticulous labour: Compared to a conventional mortar layer that accommodates deviations in the size of individual bricks, the adhesive's limited thickness cannot compensate for any dimensional discrepancies, leading to a high level of complexity in the manual bonding of the bricks and to strict dimensional controls per layer of construction (Oikonomopoulou et al. 2017). Furthermore, the permanent nature of the adhesive results in a non-reversible and non-recyclable structure.

This paper explores the potential of a novel, reversible system employing dry-assembly, interlocking cast glass components that can tackle the in-built limitations of both current systems. These include the reduced transparency which is the concomitant result of the use of a metal substructure and the irreversibility, strict tolerances and meticulous construction process of adhesively bonded systems. Interlocking systems out of cast glass components have been little explored, principally within the academic world. A realized application of the system does not yet exist. (Aurik 2017; Aurik et al. 2018; Snijder et al. 2016) have studied the concept of a dry-assembled arched glass masonry bridge where an interlocking mechanism is achieved along the longitudinal direction. (Akerboom 2016) has proposed a

---

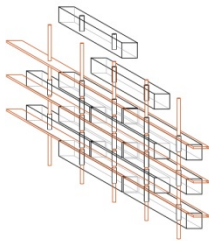
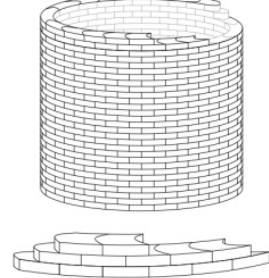
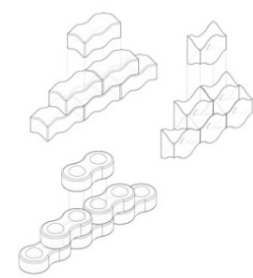
<sup>1</sup> Structures employing hollow glass blocks or solid glass blocks that are non-load-bearing are out of the scope of this research. Hollow glass blocks are generally considered non-load bearing components. Their reduced thickness results in internal buckling or stress concentrations that in turn lead to a relatively low stated resistance in compressive loading (Oikonomopoulou et al. 2017).



Figure 1: Some of the most characteristic examples of structures out of cast glass blocks: The Atocha Memorial (left) and Crystal Houses (centre), and the Crown Fountain (right)

design for an interlocking cast glass column, whereas (Barou et al. 2016; Frigo 2017; Jacobs 2017), have developed alternative interlocking glass block systems that restrain both planar directions for the transparent and reversible restoration of historic monuments (fig. 4). Besides providing an all-glass structure, an interlocking system out of solid glass elements presents several significant advantages in terms of structural performance and circularity. In principle, the overall stability and stiffness of the structure can be attained by a combination of the self-weight of the construction and the constraint of lateral movement through the interlocking geometry. The entire structure is constrained either by its own weight or by a minimised constraining frame, such as pre-tensioned tendons or cables (Dyskin et al. 2012). Furthermore, the suggested system circumvents the use of adhesives by implementing a dry, colourless interlayer as the intermediate medium between the glass units. The dry interlayer prevents glass-to-glass contact and the resulting stress concentrations. Moreover, the dry interlayer can be dimensioned to accommodate, within its thickness, the inevitable dimensional discrepancies in the cast units' size. Most important, the dry-assembly design allows for the circular use of the glass components, as they can be retrieved intact and reused. Eventually, the components can be recycled as they are not contaminated with adhesives, coatings, etc. Table 1 demonstrates the principles of the new design concept in comparison to the existing structural solutions employing cast glass blocks (fig. 2, 3).

Table 1: Principles of the different design concepts for self-supporting envelopes out of cast glass components

Additional substructure	Adhesively bonded glass structure	Interlocking cast glass units
Tensile forces are carried by an additional metal substructure	A rigid adhesive of high stiffness ensures homogeneous load transfer in the glass assembly	The structure's stiffness is obtained by the interlocking geometry of the units
		
Dry-assembly/adhesively bonded Interlayer accommodates deviations Easily assembled Compromised transparency Reversible	Adhesively bonded Adhesive's thickness cannot account for size deviations Meticulous and intensive labour High transparency Non-reversible	Dry-assembly Interlayer accommodates deviations Easily assembled High transparency Reversible



Optical House

Atocha Memorial

Proposed interlocking system

Figure 2: Brick units



Figure 3: Left: Adhesively bonded unit and system; Right: interlocking unit and system

## 2 Methodology

Cast glass interlocking components have been little explored in the past, without, so far, a consistent establishment of design criteria. Hence, initially a series of design criteria are established in respect to the principles of interlocking, the casting process, and the properties of glass. Based on these criteria, different component geometries are developed. The proposed designs are kiln-cast in 1 : 2 scale and are comparatively assessed in terms of mechanical interlocking capacity, mass distribution, generation of residual stresses and ease of fabrication. In parallel, research is conducted on different materials for the dry, transparent interlayer. A numerical model is developed for the most favourable geometries, to assess the influence of the most crucial geometrical aspects of the interlocking mechanism to the structural performance of the system, such as the amplitude and the brick height. Based on the above mentioned research results, the most promising interlocking shapes and colourless interlayer are selected in order to manufacture a dry stacked cast glass column and test it in compression. The experimental output is compared to the performance of an identical prototype employing a 5 mm thick neoprene interlayer instead.

### 3 Definition and principles of interlocking structures in architecture

An interlocking (mortarless) system consists of components that employ their geometry to ensure the kinematic constraint of the structure in one or two directions, typically the one normal to the assembly plane and its transverse. The whole assembly is stabilized by compressive forces; at times, even the self-weight of the construction is sufficient for this purpose. In such mortarless systems, the only factors that hold the components in place are weight and friction (Dyskin et al. 2012).

The concept of dry-stacked, interlocking, compressive structures is not new in architecture. Ancient Greeks had developed ingenious dry-stacked, self-aligned systems in the marble column drums of the classic temples. An example of this practice can be found in the columns of Parthenon, where the marble column drums are self-aligned with wooden pins that lock into an alcove carved in each drum (Korres 2000). Incan dry stone walls made by irregularly shaped interlocking stone polygons allowed for stable, self-aligned, mortarless structures with high seismic resistance. Roman arches and Japanese wood joinery are other proven examples of interlocking engineering.

Interlocking systems offer several advantages over traditional construction methods. Their fragmented nature allows for an increased strength and structural stability in structures made of brittle materials like glass. In particular, the segmented nature of an interlocking, dry-assembled structure leads to an enhanced fracture toughness, as cracks are confined within a block's interfaces and do not spread among adjacent elements. In contrast to a solid glass structure, failure of individual blocks does not lead to global failure. The structure can also be engineered to be sufficiently robust overall. Even if several of the units fail the rest are kept in place by the kinematic constraint from the adjusting blocks<sup>2</sup> and are able to carry the load. Enhanced stability is also achieved by the ability of the units to undergo small movements within the structure. This is particularly important to seismic zones as the interlocking structures are able to dissipate the vibration energy (Estrin et al. 2011). Compared to a mortar masonry wall, which would act monolithically against loading, a dry interlock wall allows for the resettlement of the stones, absorbing part of the seismic load in the form of kinetic energy.

---

<sup>2</sup> This principle is relevant to the specifics of the block shape and the pattern of assembly and is not valid in all interlocking geometries. E.g. in a roman arch, if the key component fails, the arch will collapse.

Equally important, an interlocking system can yield a multifunctional, easily assembled and disassembled (reversible) structure. The self-aligning nature of such structures allows blocks to fit into each other without adjustment, increasing the construction productivity and the resulting quality of the assembly. Reversibility is perhaps the most important feature in the case of glass components. According to a research made by (Eurostat 2014), glass waste is currently the second largest waste material in the European Union, even though it can be endlessly reused and recycled – provided that it is kept free of contaminants, including adhesives or coatings. A dry-assembly, reversible interlocking system promotes the dismantling of the assembly and the reusability of the components since they can be retrieved intact. Furthermore, the circumvention of an adhesive bonding and thus, of contamination, facilitates the recycling of the components.

#### **4 Design criteria**

So far, interlocking systems out of cast glass components have been little explored, principally within the academic world. A realized application of the system does not yet exist. (Aurik 2017; Snijder et al. 2016) have studied the concept of a dry-assembled arched glass masonry bridge where an interlocking mechanism is achieved along the longitudinal direction. (Akerboom 2016) has proposed a design for an interlocking cast glass column, whereas (Barou et al. 2016; Frigo 2017; Jacobs 2017), have developed alternative interlocking glass block systems that restrain both planar directions for the transparent and reversible restoration of historic monuments (fig. 4).

To this end, a thorough establishment of design criteria for interlocking cast glass structures in respect to the casting process and the nature of the material has yet to be made. Dry-stack masonry systems already exist in various materials, such as wood and stone. Given that such systems have been developed considering different manufacturing and material properties it would not be sensible to adapt the existing interlocking geometries to glass. For that reason, a series of design criteria are established for the cast glass components taking into account the principles of existing interlocking systems but reformed to fit the characteristics and peculiarities of cast glass as a construction material. These requirements are thus divided into criteria for the establishment of interlocking and criteria imposed by glass as a material and by casting as a manufacturing process.



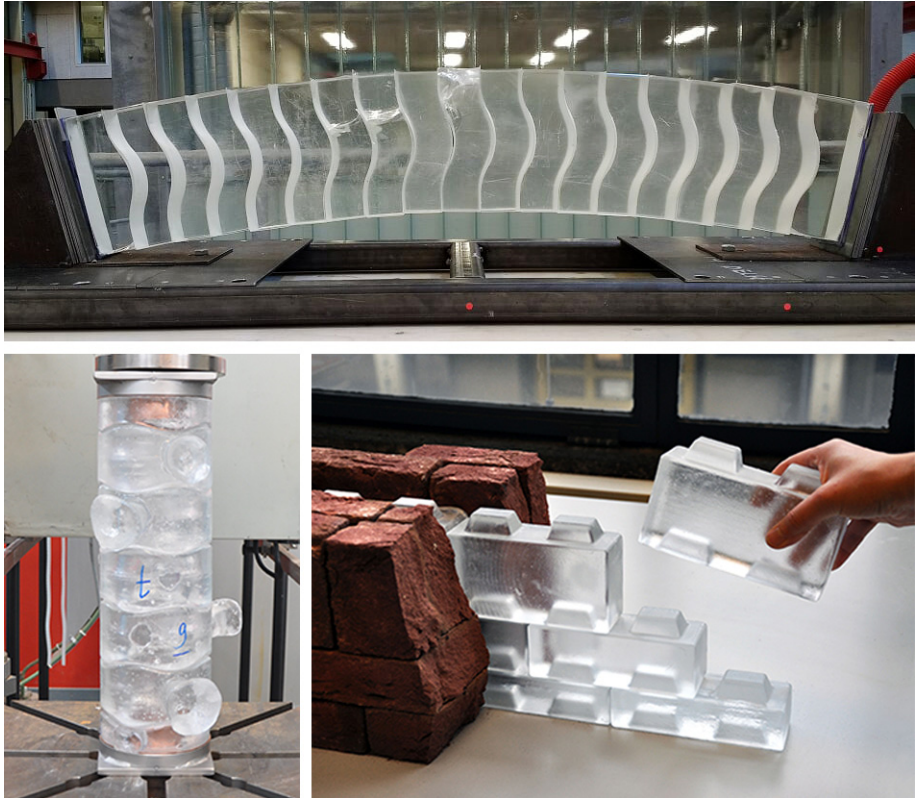


Figure 4: Interlocking glass block systems currently explored. Top: Tested prototype of the glass arch bridge by (Snijder et al. 2016). Bottom left: Glass column by (Akerboom 2016). Bottom right: Interlocking glass wall system developed by Oikonomopoulou, Bristogianni and Barou for the 3TU.bouw project Restorative Glass, presented in (Oikonomopoulou et al. 2017).

#### 4.1 Design criteria related to interlocking

Based on the principles of interlocking, the designed units should fulfil the following criteria:

- Movement confinement in both longitudinal and transverse direction

To enhance the monolithic behaviour of the assembly and ensure the desired stiffness of the structure against lateral forces, the interlocking mechanism should confine both planar direction movements. In the case of compressive structures, i.e. the ones discussed in this paper, restraint in the axial ( $z$ ) direction can be achieved either by the self-weight of the construction or by an external constraining frame.

- Optimizing shear capacity

Interlocks following smooth convex curvatures are preferred as they allow for a relatively even distribution of the shear forces occurring at the interface area. Due to the unforgiving nature of glass, traditional connectors or keys that are of a considerably smaller cross-sectional area compared to the gross cross-sectional area should be avoided as they result in concentrated stresses that can lead to premature failure.

- Self-alignment.

The interlocking mechanism should promote the self-alignment of the units, allowing for a relatively easy and fast construction of high quality. According to (Dyskin et al. 2003), convex contact areas exhibit good self-adjusting properties and also lead to reduced stress concentrations.

- Multi functionality

Towards multi functionality, a unit geometry that permits multiple configurations of stacking is preferred.

#### 4.2 *Design criteria related to glass casting*

- Limited volume

The meticulous and excessively time-consuming annealing process of cast glass can jeopardize the marketability of the components and render them financially unsustainable (Oikonomopoulou et al. 2015a). To this end, mass is a critical aspect. The larger the component, the exponentially longer the annealing time. This is well exhibited in the annealing schedule of the different block units of the *Crystal Houses* façade: solid glass bricks of 65 mm × 210 mm × 105 mm in dimensions and 3.6 kg weight required 8 h of annealing, whereas components of double the volume, i.e. 65 mm × 210 mm × 210 mm and 7.2 kg weight, required an annealing cycle of 36–38 h respectively (Oikonomopoulou et al. 2017). Even larger components can demand up to several months of controlled annealing: i.e. the *Opposites of white* drum-shaped cast sculptures by artist Roni Horn, each 50.8 cm high by 142 cm in diameter, required 4 months of controlled annealing to prevent the generation of residual stresses (Kroller-Muller Museum 2007). Hence, for this research, solid cast glass elements are designed within a 10 kg mass limitation and roughly corresponding to the size range of standard masonry units.

- Rounded shape and equal mass distribution

A rounded shape and an equal mass distribution are key aspects for the prevention of concentrated residual stresses. Curved, convex geometries are favoured over sharp, pointy edges where internal residual stresses can occur due to inhomogeneous shrinkage<sup>3</sup>. To this end, an equal cross-sectional area throughout the unit, allows it to gradually cool down uniformly, further preventing the generation of residual stresses. Subsequently, projections such as small connectors or notches should be avoided.

- Limited number of different units

A repetitive component geometry is preferred towards facilitating the production and assembly of the structure and limiting the associated manufacturing costs. A single geometry is favoured but configurations with a limited number of different elements (i.e. 2 or 3) are considered cost-effective as well. Specifically, assembly becomes easier as each unit can take any place in the structure, instead of predefined locations as is the case with systems featuring multiple geometries, such as the Incan walls. Moreover, a single geometry results in a decreased number of moulds and a standardized production process.

## 5 Interlocking designs and prototypes

Based on the above criteria, several alternative interlocking designs are developed to explore the potential of different interlocking mechanisms. The designs and block types can be seen in figure 5. Glass prototypes in 1 : 2 scale are manually produced using the kiln-cast method to comparatively assess the different designs in terms of mechanical interlocking capacity, mass distribution, generation of residual stresses and ease of fabrication. The manufactured prototypes can be seen in figures 6 to 10.

### 5.1 *Prototype manufacturing.*

For the production of the components, disposable investment moulds are produced employing the lost-wax technique. The investment slurry used is Crystalcast M248- a powder mixture of Cristobalite, Quartz and Gypsum with a maximum service temperature

---

<sup>3</sup> Edges generally cool faster due to exposure in cooling from multiple sides. In comparison, the core cools relatively slower, creating residual stresses at the edges due to this differential shrinkage. In this context, ellipsoid shapes are favourable as they allow for homogeneous cooling and correspondingly to an even shrinkage rate.

of 900 °C (SRS, 2003). Addressing the issue of recyclability<sup>4</sup>, various different glass families are used for the production of this series of visual prototypes. These include lead crystal, several soda-lime types (mouth-blown, machine-blown, float) and alkali-barium silicate. The opaque or coloured prototypes presented in the following chapter are the result of these recycling experimentations.

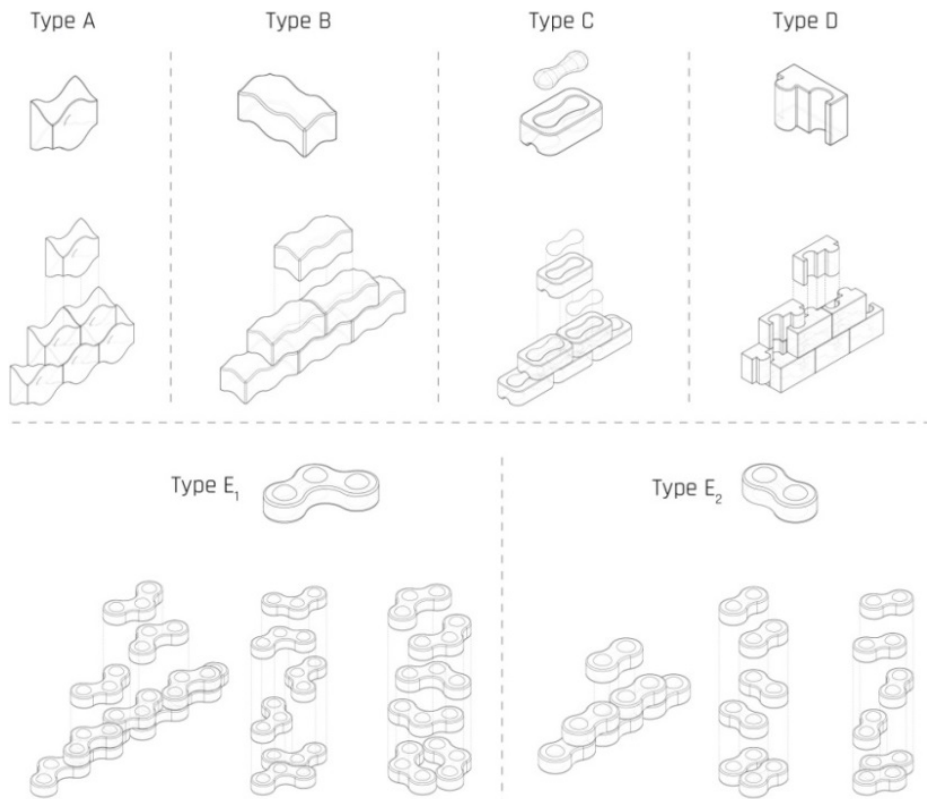


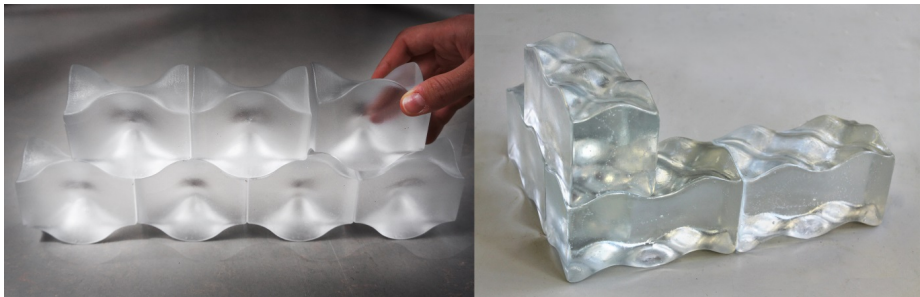
Figure 5: Developed interlocking designs

<sup>4</sup> Using waste glass for the production of safe structural cast glass components is out of the scope of this paper, yet a crucial topic of research for the authors. The results of this ongoing research are published by (Bristogianni et al. 2018).

## 5.2 *Interlocking geometries*

- Types A & B: Osteomorphic blocks

Type A and B blocks (fig. 6) follow an osteomorphic geometry as defined by (Dyskin et al. 2003). These shapes have been engineered with non-planar concavo-convex surfaces. The convex parts of the surface of one element match the concave parts of the other and vice versa. In this way, relative movements in both planar directions are impeded, provided that the assembly is constrained at the periphery. A benefit of the osteomorphic shapes is – given that the contact surfaces are sufficiently smooth – the generation of mild stress concentrations compared to the ones produced by conventional interlocking connectors or keys (Dyskin et al. 2003). In the developed designs, the symmetry of the interlocking unit in the x and y axis allows the use of the same component parallel or perpendicular to the one placed below. Thus, corners can be easily obtained with the same block unit. The assembly of the structure can be easily realised by stacking the blocks on top of each other. Only the blocks on the periphery need to be separately constrained.



*Type A*

*Type B*

*Figure 6: Osteomorphic blocks*

- Type C: Two-component interlock

In this system interlocking is achieved through matching male and female components. This design provides more freedom in terms of material use and visual aesthetics. For example, one component geometry can be made of glass and the other can be made of another material, e.g. metal, plastic or coloured glass as shown in figure 7. Materials can also be selected to match the stress distribution of the mechanism; it is anticipated that stresses will not be evenly distributed in both components due to the difference in geometry: Annealing is considered to be homogeneous for the bone-shaped component because of its relatively even mass distribution and ellipsoid ends. The block-shaped

component requires a more meticulous annealing cycle to prevent internal residual stresses due to its relatively inhomogeneous cross-section (solid in the middle, with cavities at the edges). This design does not allow for the creation of corners in the structure with the same elements, due to the block's non-symmetrical interlock in the transverse direction, calling for the design of additional elements. A peripheral constraint is necessary for further stabilizing the structure.

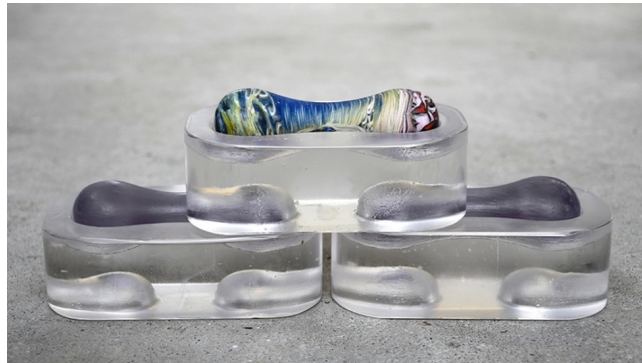


*Figure 7: Type C Prototype. The bone-shaped components are made of recycled coloured glass.*

- Type D: Puzzle brick

This design follows a different interlocking mechanism than the ones previously described: here, the components slide vertically to each other. In particular, the components are positioned halfway in height and width in relation to their adjusting components (fig. 8). In this fashion, continuous joints -weak zones susceptible to stress concentrations- are



*Figure 8: Type D prototype made of clear glass, recycled float glass (teal) and recycled Cathode Ray Tube (CRT) screen (black)*

prevented. Compared to the aforementioned interlocking mechanisms, this system restricts the self-alignment of the bricks in both planar directions and thus, decreases its damping properties. In addition, the relatively complex shape of this unit may result to internal residual stresses during the annealing of the cast element, as well as to local stress concentrations during loading. As with type C, due to the unit's asymmetrical interlocking mechanism, corners employing the same component cannot be achieved in the structure.

- Type E: Rotational brick

The almost semi-spherical key of this geometry provides further flexibility in the form of the overall assembly compared to the previous solutions. For example, the same modulus can be used to make either planar or cylindrical structures. The two different block types (E1 and E2) can also be combined together to create one structure (fig. 9). The curved geometry of these block types can guarantee a satisfactory homogeneous annealing. However, the considerable projections of the semi-spherical connections may result in local shear stress concentrations during loading.








*Figure 9: Prototype using E1 and E2 glass blocks from clear glass and recycled mouth-blown coloured glass*

A comparative assessment of the presented interlocking designs based on the established design criteria can be seen in Table 2.

Out of the established designs the osteomorphic blocks (types A, B) are considered by the authors to be the most promising elements for further development due to their multi functionality, ease of assembly and ability to prevent peak stress concentrations, both during the casting process and during loading. The smooth curves and even mass

Table 2: Comparative assessment of the different interlocking block types based on the established design criteria

Block type	A	B	C	D	E
Interlocking mechanism					
Interlocking mechanism	smooth curves	smooth curves	male and female blocks	sliding blocks – intense curves	semi-sphere keys for vertical stacking – ability to rotate
Shear capacity	high	high	moderate	moderate	moderate to high
Self-alignment	high	high	high	low	high
Multi functionality	high	high	moderate	moderate	high
Equal mass distribution / homogeneous annealing	effective	effective	risk of internal residual stresses	risk of internal residual stresses	effective
Lim. number of dif. units / ease of assembly	high	high	moderate	moderate	high



distribution of the components allow for their homogeneous annealing preventing the generation of internal residual stresses. The smooth concave-convex interlocking mechanism of the elements ensures its high shear capacity as well. Even though stress concentrations may occur to the concave parts of the surfaces upon loading, these are likely to be mild compared to the ones occurring in small keys or connectors (Dyskin et al. 2003). The system also has high damping properties: restricted movements of the blocks relative to each other are still possible, allowing for self-alignment and dissipation of energy in case of seismic loading. Moreover, the redundancy of this type of blocks has been proved before by (Dyskin et al. 2003). Such a system is highly tolerant to local failures and it has been demonstrated that after the collapse of random blocks the structure can resist by percolation of damage until nearly 25% of block failure. Lastly, in terms of multi functionality, the symmetry of the developed osteomorphic blocks in both planar directions allows their assembly in configurations with 90° rotations, achieving for example columns and wall corners (fig. 10). Half-blocks are necessary to finish the edge of the structure.

## 6 Dry interlayer

Dry-stacked glass under axial load is never expected to fail due to its compressive strength limit. Due to the inability of glass to deform plastically, any unevenness or imperfections at the contact surface of the components can introduce local high tensile stresses. The inherent brittleness of glass can respond to such peak stresses with crack propagation and

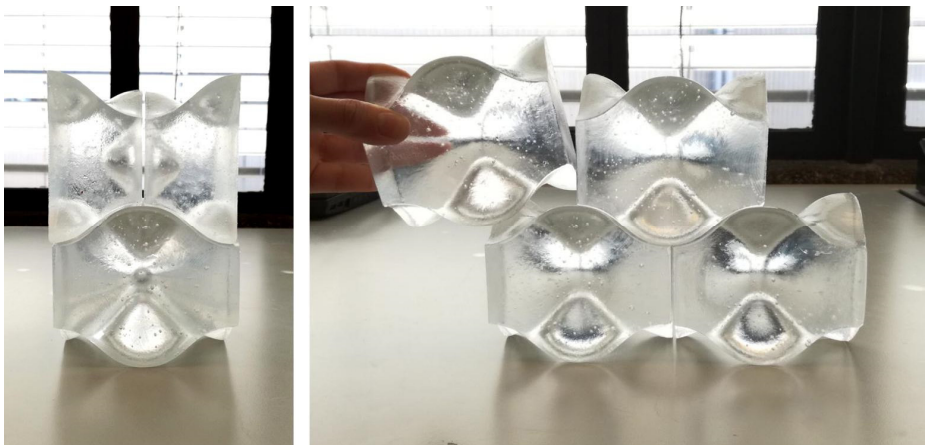


Figure 10: Possible structural geometries using osteomorphic blocks (Type A)

eventually failure. This has been demonstrated in cast glass by axial compressive tests by (Oikonomopoulou et al. 2015a) performed on annealed soda-lime glass bricks with direct contact to the steel surface of the testing machine. The specimens failed in an average nominal compressive stress of 20-30 MPa, values close to the stated tensile strength of annealed glass. A resilient dry interlayer is thus essential for accommodating by deformation surface asperities and for evenly redistributing the stresses on the contact area. The application of an interlayer can, however, decrease the stability of the overall structure. Hence, suitable interlayers lie within a certain stiffness interval. I.e. harder polyurethanes have an increased stiffness and incompressibility, which affects the spreading of the stresses negatively and decreases the tolerance for imperfections in the contact surfaces. Thus, in order for the interlayer to accommodate dimensional discrepancies, the interlayer should have a considerably lower elasticity than glass. According to (Aurik et al. 2018) polymers, with a Young's Modulus between 0.2-5 GPa are a promising candidate.

In addition to the above, the main criteria for an interlocking, dry-stacked, application are the behaviour of the material under long-term compressive loads, its time-dependency response and creep resistance. Besides these properties, the following requirements are considered for the selection of the interlayer:

- Transparency and durability to UV-lighting
- Good behaviour under static long-term compressive load
- A compressive strength higher than 10 MPa
- Ability to be formed in a consistent thickness in the desired shapes
- A consistent thickness of at least 2-3 mm to accommodate dimensional discrepancies
- A maximum service temperature of 50° C

According to CES Edupack 2015 program (Granta Design Limited 2015) the following thermoplastic and elastomer polymers fulfil the above-mentioned criteria:

- PEBA - Polyether block amide
- PU - Polyurethane (rubber/cast)
- PVC - Polyvinyl Chloride (soft)
- TPU - Thermoplastic polyurethane

These materials can be processed to the desired shape either by injection moulding or extrusion. PU, PVC and TPU have already been applied in the building industry. TPU, which is used as well in laminated glass, only obtains its mechanical properties after it has been thermally processed; thus it is not considered appropriate for this study.

Subsequently, PU rubber and soft PVC are considered the most suitable materials.

Experimental work by (Aurik et al. 2018) in PVC, PU70 and PU90 proved that PVC's E-modulus is strongly time-dependent and creep occurs under static loads. Moreover, there is discoloration (to a yellow hue) of the material after long UV-exposure. Therefore, PVC is considered unsuitable for the purposes of this research. Experiments of (Aurik et al. 2018) with PU70 proved that its time dependent behaviour is not significant. In PU, a thicker interlayer, desirable in the presented application for the accommodation of size deviations, is equivalent to a larger modulus of elasticity. The experimental results were inconsistent for PU90 and showed an irregular pattern of contact area under high compressive loads. Hence, among the analysed samples, the most promising material for the dry interlayer is considered to be PU70 rubber which can be cast to the desired shape in a uniform thickness. A prototype of a 3 mm thick, cast PU70 interlayer, manufactured for the type A blocks, can be seen in figure 11.

## 7 Optimization of the interlocking geometry of the osteomorphic blocks by numerical modelling

### 7.1 Model set-up

As discussed in chapter 5, interlocking blocks following an osteomorphic geometry are selected by the authors as the most promising components for dry-assembled interlocking glass structures. To further assess the influence of the most crucial geometrical aspects of the interlocking mechanism, namely the amplitude and the brick height, on its performance and structural capacity, a numerical model is made for block types A, B<sup>5</sup> with brick dimensions of 300 x 150 x 150 mm. A detailed description of the model set-up can be found in (Jacobs 2017). The geometry of the block is generated through the Grasshopper plug-in for Rhinoceros. This plug-in allows for automatic generation of new geometries by

---

<sup>5</sup> A more detailed study regarding the presented numerical model can be found in (Jacobs 2017). The numerical model has been developed for type B block but corresponds in both types, since Type B block is generated by multiplying Type A. It is expected that compared to type B, type A blocks will present a slight decrease in load capacity due to extra eccentricity in loading.



Figure 11: Prototype of a 3 mm thick, cast PU70 interlayer

changing certain input parameters. The model variations<sup>6</sup> are then exported as a solid, using a STEP-file and imported into DIANA FEA, a finite element software.

The variation models are evaluated using the Christensen's failure criterion output, which essentially converts the principal stresses and its material properties into a failure envelope definition, including a limitation for the tensile capacity of brittle materials (Christensen 2013). Loading the interlocking brickwork in shear, the generated contour plots show how tensile peak stresses are spread on the contact surface (fig. 12). Hence these contour plots

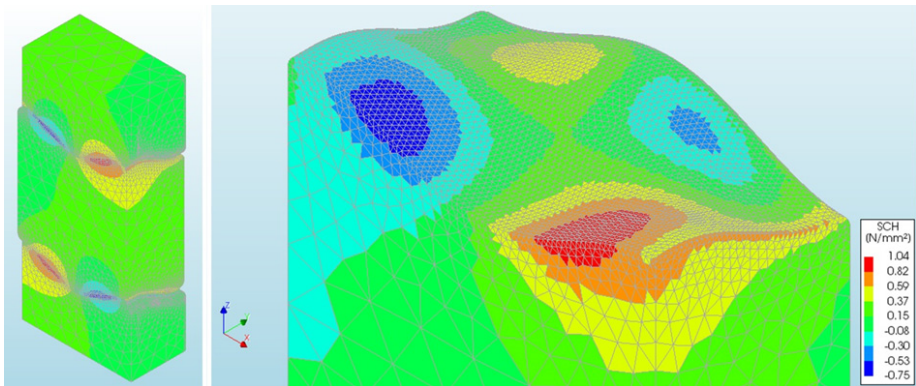


Figure 12: Left: Numerical set up and results for Christensen's failure criterion value of one (SCH=1) of the tested variants. Right: Christensen's output (SCH=1) of middle brick (amplitude 10 mm). Shear capacity at failure is approximately 155 kN.

<sup>6</sup> Shape deviations due to fabrication tolerances in the size of the unit were not considered in the final model.

can be used to indicate: 1) where flaws in the geometry would be most influential (tensile opening of cracks); 2) how stress concentrations spread onto the contact surface; and 3) the stress gradient at sections in the geometry. By evaluating both the contour plots and the shear lock capacity multiple geometry variations can be evaluated on their applicability as cast glass interlocking components. The numerical model showed that any compressive load puts the geometry in a compressive state and hence yields higher shear capacities compared to when no compressive force was applied. Hence all variants were tested without any compressive load; instead the shear-load-inducing bricks were constrained in the global z-direction.

### 7.1.1 Geometry set-up.

By using the symmetry of the Type B brick design the whole model can be reduced to a quarter of its original size. This leads to fewer elements and a more efficient calculation time. Thus, to mimic a shear test, one quarter of a brick is held between two eighth bricks; in-between the glass elements two 4 mm thick PU interlayers are placed. Figure 13 shows a full-scale principle of the DIANA model in 2D.

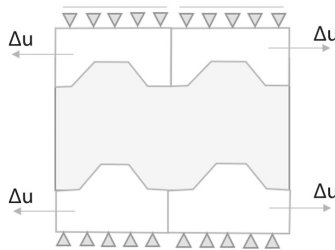


Figure 13: 2D Full scale principle of the model

### 7.1.2 Material settings

The used values for Poisson's ratio and Young's modulus are calibrated using experimental research by (Aurik et al. 2018)<sup>7</sup> and hence are only valid for a PU with a hardness of 70 Shore A. The input properties can be found in Tables 3 and 4.

---

<sup>7</sup> A detailed explanation of the calibration method can be found in (Jacobs 2017). To calibrate the Young's modulus of PU to a realistic value, part of the test set up discussed in (Aurik 2017) is modelled in DIANA FEA. A fine mesh with element size of 2 mm is applied on the PU interlayer, and to limit calculation time and file size the mesh size is gradually increased to 20 mm. A compressive distributed load of 10.88 MPa is applied on the top glass face to conform the test setup discussed in (Aurik 2017). The Young's modulus is

Table 3: Input properties of glass and polyurethane interlayer

Material	Glass	Polyurethane
Density	$2.5 \cdot 10^{-9} \text{ t/mm}^3$	$1.1 \cdot 10^{-9} \text{ t/mm}^3$
Poisson's ratio	0.22	0.48
Young's modulus	70000 N/mm <sup>2</sup>	50 N/mm <sup>2</sup>
Tensile strength	45 N/mm <sup>2</sup>	-
Compressive strength <sup>8</sup>	360 N/mm <sup>2</sup>	-

Table 4: Input properties of interface elements

Parameter	Value	Unit
Cohesion $c$	0.001	N/mm <sup>2</sup>
Normal stiffness modulus $z$	$70 \cdot 10^6$	N/mm <sup>3</sup>
Shear stiffness modulus $x$	$7 \cdot 10^6$	N/mm <sup>3</sup>
Shear stiffness modulus $y$	$7 \cdot 10^6$	N/mm <sup>3</sup>
Tensile strength gap criterion $f_t$	0.0005	N/mm <sup>2</sup>
Friction angle $\phi$	1.1	rad
Dilatancy angle	0	rad
Interface opening model	Gapping model	-

### 7.1.3 Support conditions

A scheme of the support conditions can be seen in figure 15. The main intention of the model is to calculate the shear capacity of the interlocking geometry. The most critical brick is expected to be in the top of the construction, where the least vertical loading is present. Thus, one desired result of the model is to obtain the force necessary to prevent uplifting. Figure 14 shows the principle of uplifting in the studied geometry.

then varied until a deformation of 0.13 mm is found, corresponding to the result of the laboratory test. The results suggested a value of  $E = 50 \text{ MPa}$  with a Poisson's ratio equal to  $\nu = 0.48$ .

<sup>8</sup> For the tensile strength (T) of glass the characteristic strength of annealed float glass is used. Christensen states that  $T/C = 1/8$  for glass, thus, its compressive strength (C) is set to 360 MPa. In reality the compressive strength of glass can be significantly higher, but to satisfy the Christensen criterion the earlier mentioned value is applied in the model. As the leading fracture mechanism in glass occurs only due to tensile peak stresses it is not necessary to excessively review the influence of compressive stresses on the geometry.

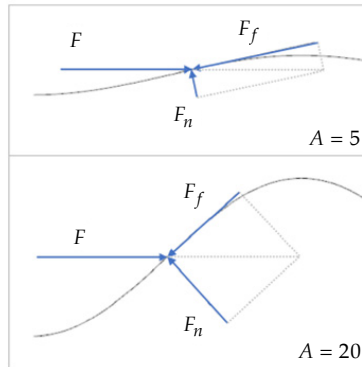


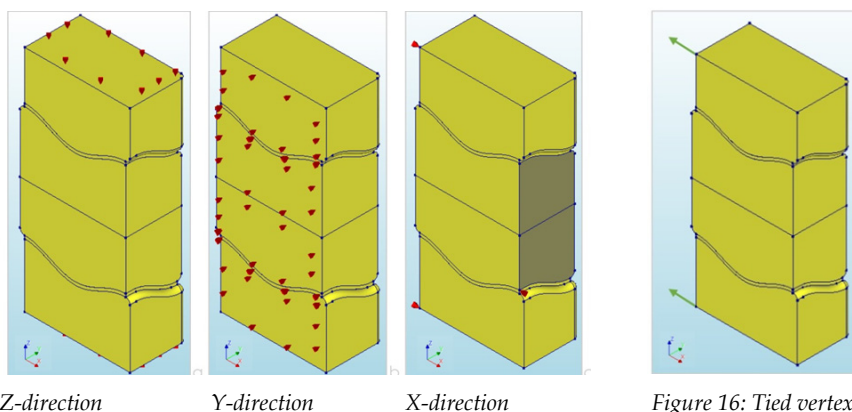
Figure 14: Principle of uplifting for interlocking blocks with amplitudes of  $A = 5$  mm and  $A = 20$  mm. The shear force is depicted as a concentrated force ( $F$ ) halfway the amplitude. Dead weight and weight of upper structure are not accounted for. The force is conveyed in two directions: To an uplifting force ( $F_f$ ) by traction parallel to the steepness at that point and to a force ( $F_n$ ) by compression normal to the geometry.

To evaluate the uplifting behaviour, the upper and bottom plane of the assembly are restraint in the Z direction. Due to the shear loading it is expected that parts of the geometry will want to move upward, creating reaction forces across the planes. In the Y-direction supports are added to simulate the symmetric geometry of the type B block. The sliced face is thus restraint in the Y-direction. In the X-direction, a similar support is needed for the middle block. One vertex is supported here which is tied to shaded faces. In this way, any deformation set in any node of these faces will have the same deformation as the master node. All reaction forces are summed into this master node, which enables easy access to the desired value of the characteristic shear strength of the geometry. Two more supports are added in the X-direction for the top and bottom bricks, to accommodate the prescribed deformation loads that introduce the desired shear loading of the assembly. Again the nodes are tied to the future mesh nodes on the corresponding surface, gaining supports and the same prescribed deformation.

#### 7.1.4 Loading conditions

As previously mentioned, a prescribed deformation is applied to the top and bottom blocks. Owing to the sliding support on top and bottom, these geometries are free to move, with only the interlocking geometry as obstacle. The applied load is conveyed through the PU interlayer to the middle block, which will in turn display the resulting stress

concentrations according to Christensen's failure criterion. The load is applied on the supported vertexes, which due to the tying will copy the same deformation to any of the nodes on the tied surface. A prescribed deformation of  $\Delta u = -0.1$  mm is applied to both vertexes (fig. 16).



Z-direction  
Y-direction  
X-direction  
Figure 15: Support conditions

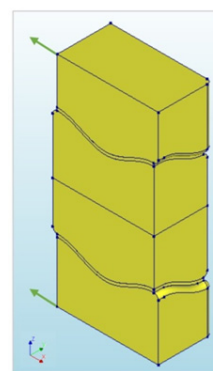


Figure 16: Tied vertexes loaded with a prescribed deformation load

### 7.1.5 Parameter ranges tested

A selection of models with different amplitude and height variants are generated and tested in DIANA. The initial model is set with an amplitude of 10 mm and a height of 150 mm. The tested amplitudes are in a range from 5 mm to 20 mm. The parameter variations for the height are between 40 mm and 150 mm. Higher bricks than 150 mm would be considered impractical in terms of installation and fabrication, as the initial brick design is already approx. 17 kg in weight.

## 7.2 Results

Figure 17 gives an overview of the influence of different amplitude and brick height variants on the shear capacity. Figure 18 demonstrates that a higher amplitude would increase the shear capacity due to a larger contact area for the stresses to spread on, while reducing the relative uplifting behaviour. A higher amplitude would also increase the chances of a shear-key failure, which is considered beneficial as it provides a warning failure mechanism. As can be depicted from the contour plots in figure 19, the tensile and compression areas grow in horizontal direction in the shear keys. This increases the probability of a shear key failure instead of a splitting brick failure. A negative effect of an



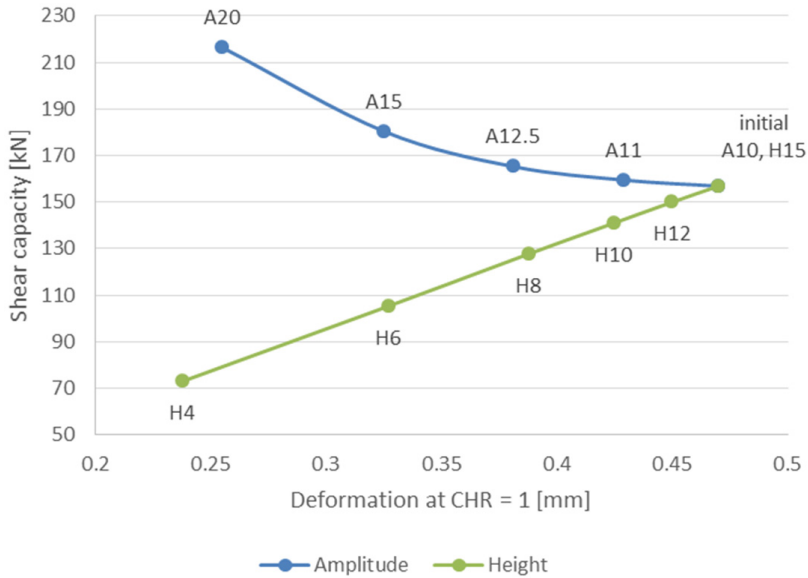


Figure 17: Shear capacity and deformation at failure of the different variants

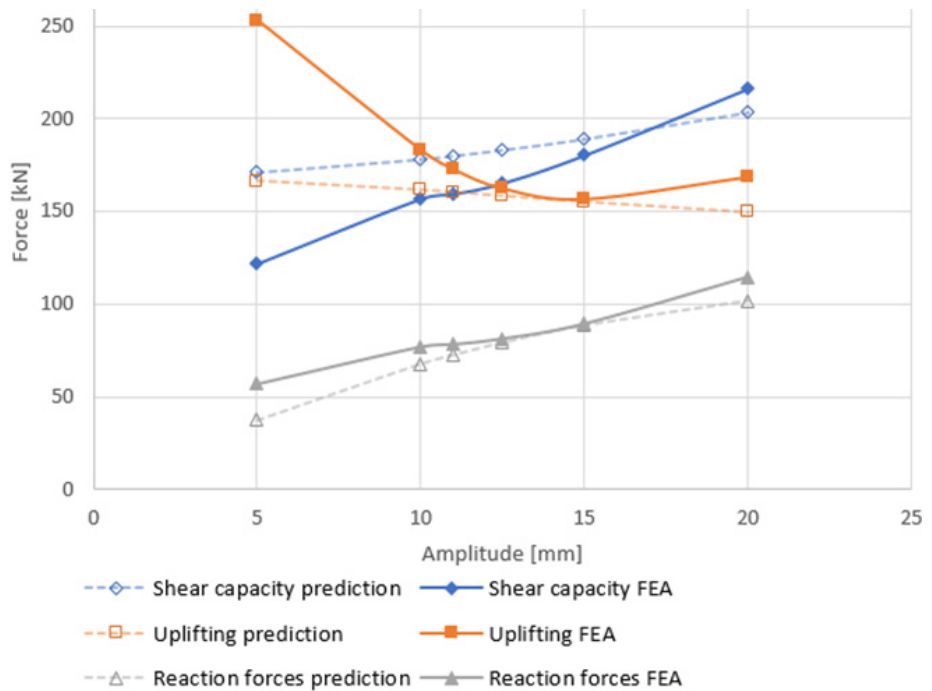


Figure 18: Influence of amplitude on shear capacity, uplifting force (parallel to interlock curvature) and reaction forces. The prediction lines are based on hand calculations described in (Jacobs 2017).

increase in amplitude is that a higher precision of the brick geometry is required, as the failure limit is reached at a smaller deformation (fig. 17). A deviation from the perfect geometry<sup>9</sup> would hence lead to earlier failure for brittle materials (as also discussed by (Dyskin et al. 2003)) compared to lower amplitude variations. An excessively small amplitude however would result in uplifting to become a crucial factor, needing a heavier top constraint and relying more on friction than on the interlocking geometry. The choice for a higher amplitude is therefore considered a trade-off between a higher shear capacity and a reduction in uplifting behaviour on the one hand, and geometry precision on the other hand.

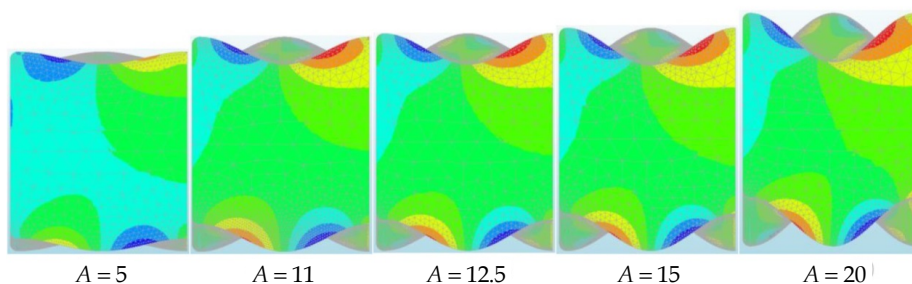


Figure 19: Contour plots at failure load for various amplitude variations, demonstrating the stress redistribution of the given geometries. For the failure loads of each amplitude variation refer to figure 17.

Figure 20 exhibits the influence of the height of the brick on the failure mode of the glass brick. The graph shows failure through bending to be critical in lower brick heights (in this case less than 80 mm in height) as they are subject to higher stresses due to eccentric loads. Higher variants are more resistant to this, leading to shear key failure. These failure mechanisms are expected to occur in the most flaw-prone area, as derived from the Christensen's failure criterion. Thus, the upper boundaries were determined from a simplified hand calculation using the characteristic strength of glass. It is expected that the real value lies somewhere below, as the combination of the principal stresses in the Christensen's criterion lead to failure before reaching this characteristic value. Thus, figure 20 incorporates the results from the finite element analysis versus the simplified hand calculations. Regarding geometry tolerances, higher bricks are also advantageous, as the

---

<sup>9</sup> As a reference, in current adhesively-bonded cast glass applications, cast glass blocks are made with fabrication tolerances ranging between  $\pm 0.25$  mm (Oikonomopoulou et al. 2015b) to  $\pm 1.00$  mm (Goppert et al. 2008).

failure load occurs at a larger deformation. This means a larger geometry deviation is allowable when producing the interlocking bricks when compared to thinner bricks. Hence a higher brick is beneficial for brick design, as capacity is increased, tolerances can be slightly higher and there is an increased chance on the preferred failure mechanism: an interlock chipping off would leave the remainder of the brick intact for increased structural integrity.

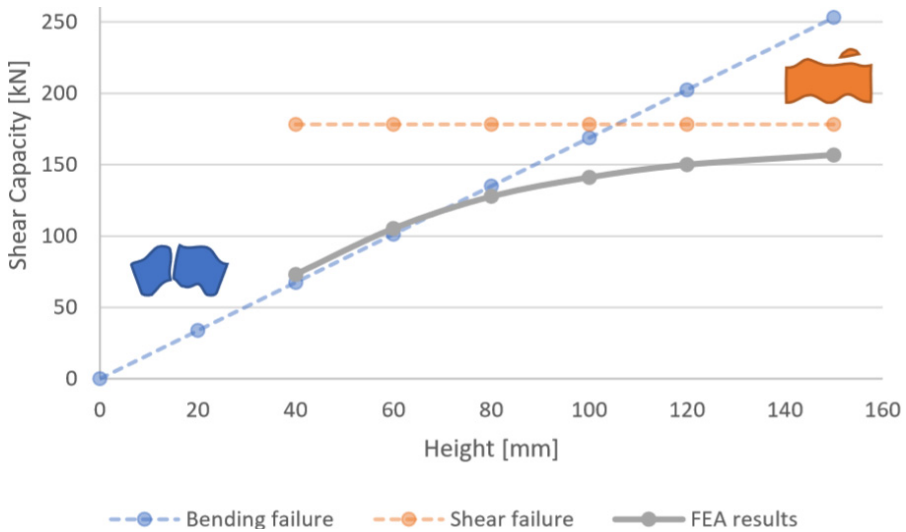


Figure 20: The effect of the height on the shear capacity of the brick plotted together with the expectations from hand calculations

## 8 Experimental investigation of osteomorphic blocks-interlayer system

Based on the above findings, it was determined to further investigate the performance of a dry-assembly, interlocking system utilizing osteomorphic blocks (type A) with two different interlayers: (1) cast PU70 interlayer of 3 mm thickness and (2) neoprene of 5 mm thickness. Neoprene, although non-transparent is often employed as an interlayer in structure out of brittle materials and can thus be used to set a good reference basis.

### 8.1 Materials

A series of osteomorphic blocks, each measuring 52.5 mm x 100 mm x 91.3 mm, were kiln-cast using disposable Crystalcast M248 moulds at the TU Delft Glass & Transparency lab facilities. Schott B270 modified soda-lime glass was employed for the production of the

glass components. The blocks were cast at 940 °C and then annealed between 540 °C and 510 °C. The complete kiln-casting and annealing schedule can be seen in figure 21. Afterwards, the prototypes were ground and polished with a Dremel rotary tool with diamond pads, to eliminate possible imperfections at the interlocking surfaces. Regarding the PU70 interlayer, a two part 3D-printed mould out of Polylactic acid (PLA) was used in order to cast the PU resin into the appropriate interlayer shape. The characteristic properties of the PU and neoprene interlayers can be found in table 5.

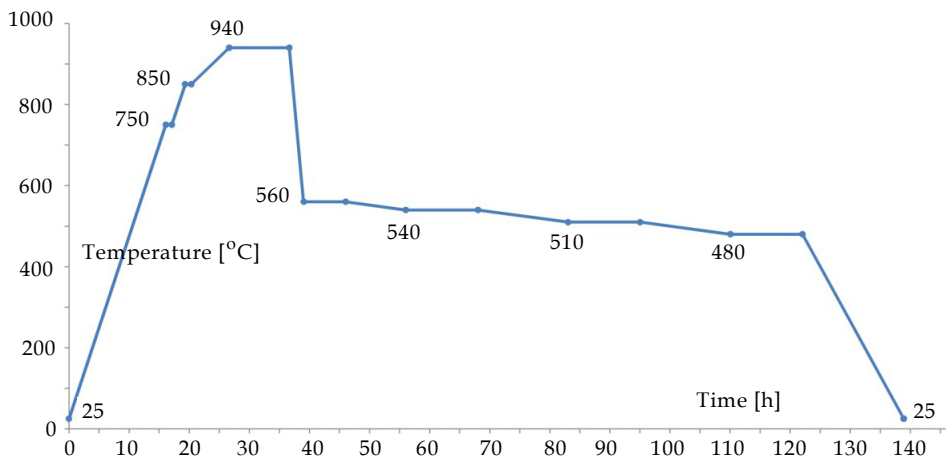


Figure 21: Firing schedule followed for the kiln-casting and annealing of the osteomorphic blocks

Table 5: Characteristic properties of neoprene and PU70 as derived from (Aurik et al. 2018; Granta Design Limited 2015). Thickness is not given for the presented values.

Property	Unit	PU70	Neoprene
Shore hardness	Shore A	70 ( $\pm 5$ )	45 - 85
Gross density	g/mm <sup>3</sup>	1.24	1.35 - 1.5
Poisson's ratio	-	0.48	0.48
Young's modulus	GPa	0.002 - 0.015	0.0025 - 0.03
Compressive strength	MPa	12.6 - 25.6	48 - 61.2
Tensile resistance	N/mm <sup>2</sup>	$\geq 40$	11.4 - 21.3
Elongation at breaking	%	$\geq 550$	120 - 780
Tear strength	N/mm	60 - 90	27 - 56
Flexural strength	MPa	65 - 81	22.6 - 37.3

### 8.2 Set-up

Two specimens, each consisting of 7 osteomorphic blocks (5 whole and 2 half components forming the bases) were tested in compression with a Zwick100 Machine with a speed of 5 mm/min. Each specimen measures 52.5 mm x 100 mm in plan (fig. 22). Specimen A is 570 mm high and Specimen B is 582 mm high due to the difference in the interlayer thickness: In specimen A, a cast PU70 interlayer of 3 mm thickness was placed between the blocks as the intermediate medium to prevent glass to glass contact. In specimen B, neoprene of 5 mm thickness was applied instead. Both specimens had a slight eccentricity from the vertical axis due to the manufacturing tolerances of the manually made components. The set-up for each specimen can be seen in figure 23. An additional neoprene interlayer was placed at the top and bottom of each specimen to prevent direct contact of glass with the steel surface of the testing machine. A large wooden block is placed between the head of the machine and the column to level and absorb the initial deformations of the contact surface.

### 8.3 Results

The force-displacement graph of the experiments can be seen in figure 24. The initial ductile deformation is attributed to the adjustment and deformation of the wooden block placed between the head of the machine and the glass specimens.

The experiment of Specimen A was stopped in a compressive force of 32700 N due to failure by splitting of the wooden block. Once the experiment was interrupted, it was

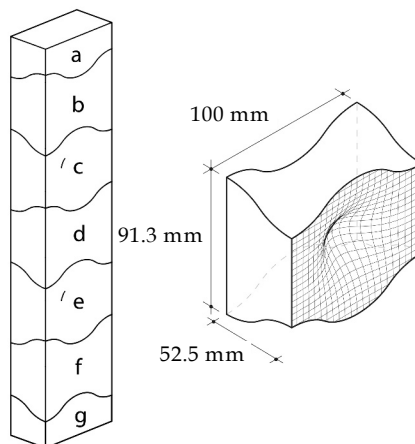
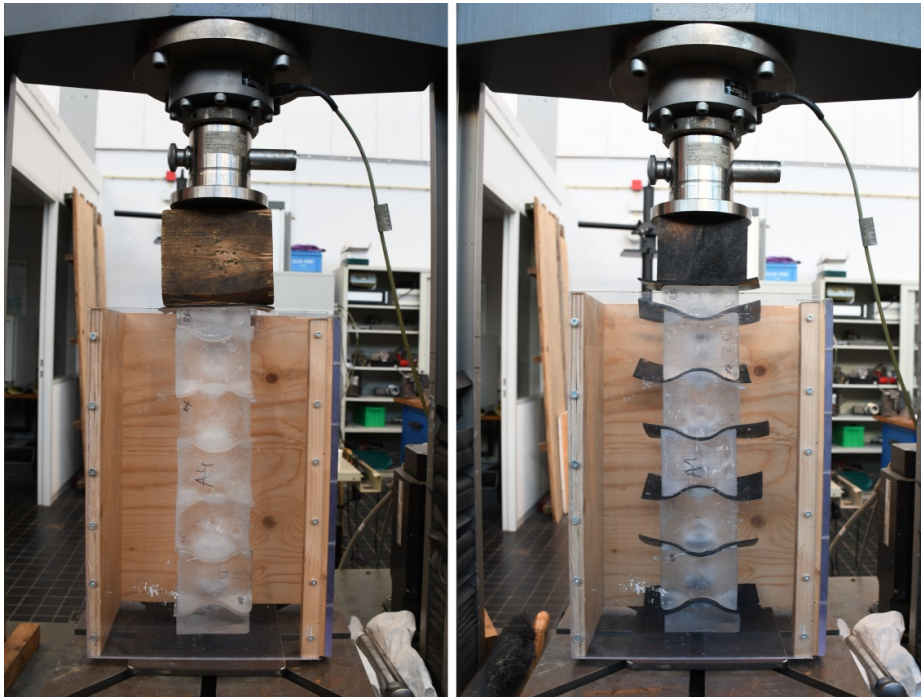


Figure 22: Specimens' composition and dimensions of individual component



Specimen A

Specimen B

Figure 23: Specimens prior to testing

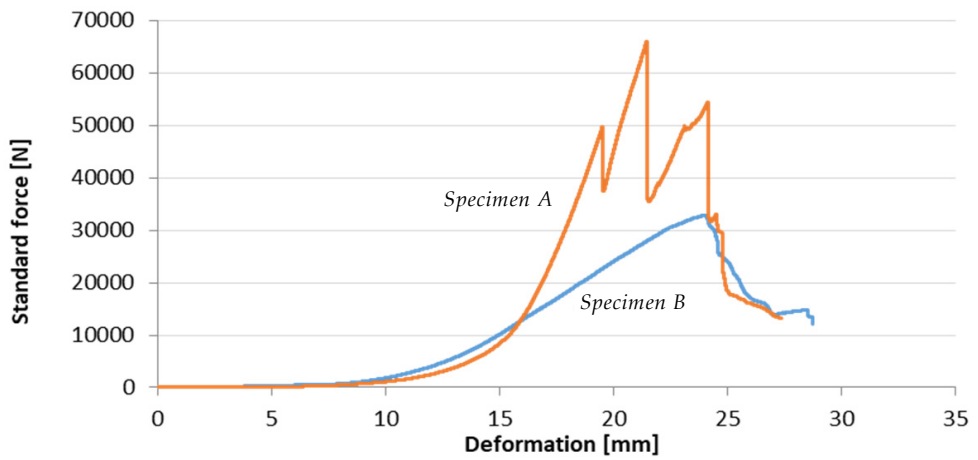


Figure 24: Force-displacement diagram of specimens A (blue) and B (red)

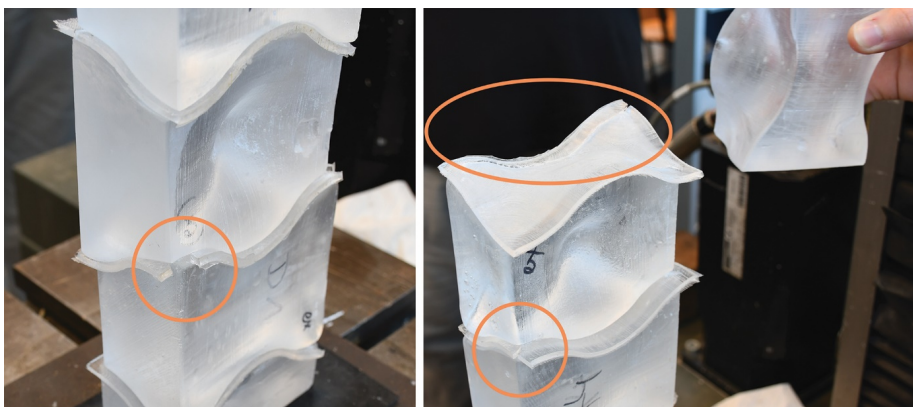


Figure 25: Failure of the PU70 interlayer in Specimen A

observed that the cast PU interlayers had been torn by the glass components (fig. 25), leading to a direct contact of the glass blocks which in turn resulted to the chipping of the edges of blocks c and e due to induced localized (tensile) stresses. Because of the preliminary failure of the interlayer it was decided to not continue the test.

A new, harder wooden block was used to test Specimen B. The specimen failed completely at a compressive force of 66956 N, possibly due to induced bending stresses. Initially a crack appeared to the top block (a), then the third block from the top failed (c), followed by cracks to the one above it (b). Finally, block d chipped off at one corner (fig. 26). The chipping can also be a result of earlier than anticipated failure due to residual stresses because of improper annealing of the edges of the specimen. The bottom three components (e, f, g) remained intact.

#### 8.4 Discussion

The limited number of specimens suggests that the experimental data are not sufficient for statistical purposes and cannot be considered conclusive for establishing mechanical properties. Still, they highlight several important aspects of the interlocking dry-assembly system. In particular, both specimens exhibit an increased fracture toughness, preventing cracks propagating from one brick to another. In particular, in both specimens there was no subsequent crack failure among adjacent bricks observed. Instead, as the load increased, cracks would appear in blocks apart from each other.





*Figure 26: Specimen B after failure. Left: overview; Right: crack patterns in blocks a, b and d (top down). Block c was completely fragmented and could not be retrieved after the testing.*

The increased fracture toughness also results in an increased redundancy of the assembly. The dry-stacked columns could still carry a considerable amount of the total load after some of the components were broken, providing a warning prior to catastrophic failure. This is as well illustrated in figure 24 where the low peaks at the graph line of specimen B indicate the cracking of the individual blocks. Subsequently, it is expected that a dry-assembly glass wall following the proposed interlocking geometry will exhibit sufficient redundancy and resist collapse as also suggested by the work of (Dyskin et al. 2012) on osteomorphic blocks cast from polyester resin PolyLite 61-209.



The assembly exhibits a lower bending stiffness and load-bearing capacity than the one expected in a monolithic component. Both of these aspects can be explained by the fragmented nature of the assembly (Dyskin et al. 2003). The failure mode of the blocks in Specimen B indicated bending stresses to be the dominant failure mode, which is anticipated due to the loading scheme (in compression) and set-up of the experiment. It is also expected that, due to the manual fabrication of the components, a larger amount and size of flaws exist in the components that may have contributed to an early failure compared to components made by a standardized, highly controlled production.

The tearing of the PU70 interlayer in a load  $< 32$  kN in Specimen A is a contradictory result taken into account the higher flexural and tear strength of PU compared to neoprene and the experimental findings of (Aurik et al. 2018). It is considered by the authors that there may have been a slight error in the mixing ratio of the components during the casting recipe of the PU interlayer, resulting in a less stiff interlayer with decreased properties. Still, the result indicates that an interlayer of increased shear strength is necessary to prevent early failure due to the tearing of the interlayer as was the case with the tested PU70. In comparison, specimen B could carry almost double the load prior to failure due to bending stresses.

## 9 Conclusions

Based on the established design criteria, several different designs and interlocking mechanisms are developed. Physical prototypes of each design are kiln cast in 1 : 2 scale. The assessment of the prototypes by the formed criteria suggests that blocks following osteomorphic interlocks are the most promising solution for cast glass components: they present an equal mass distribution, homogeneous annealing, multi functionality, high shear capacity and damping properties. A further assessment of this type of blocks through numerical modelling gives valuable input regarding the influence of the geometrical parameters of the interlocking geometry in the overall structural performance in shear. In specific, a decrease in the height of the blocks lowers its shear capacity and alters the system's failure mechanism: a lower brick is more susceptible to bending, whereas for higher brick variants the shear lock failure is proven to be more critical. Both failure mechanisms are nevertheless still possible, even for higher bricks, as peak tensile stresses occur at the middle of the block. A flaw in that area could lead to crack propagation normal to this region. It was also proven that an increased amplitude of the

interlock can be beneficial as it leads to an increased shear capacity and lower uplifting effects. Nonetheless, increased amplitudes also require a higher manufacturing precision as the components can reach the failure stress limit in considerably smaller deformations.

Research on different interlayer materials suggests that PU fits best for the presented dry-assembly glass application in terms of structural performance and shaping potential. The ability to cast PU allows the generation of interlayers of consistent thickness and of perplex curved geometries; such as the ones needed to match the interlocking surfaces of the osteomorphic blocks. The experimental testing in compression of a dry-stacked specimen comprising osteomorphic blocks with a 3 mm thick PU70 cast interlayer as an intermediate medium was considered inconsistent by the authors for deducting further conclusions. The unexpected early failure of the interlayer due to tearing is contradicting the higher flexural and tear strength of the material compared to neoprene. Thus, it is anticipated that there may have been an error in the mixing ratio of the PU components during casting that significantly altered its properties. Specimen B, comprising a 5 mm thick neoprene interlayer failed due to induced bending stresses in the glass components. Thus, further research is essential in the direction of a colourless interlayer of sufficient UV stability, stiffness, shear and tear strength.

## 10 Further work

Further research will focus on the experimental validation of the selected designs in order for statistical data to be derived, as well as on the effect of pre-compression as a peripheral constraint structure. A more in-depth experimental work is necessary to evaluate the mechanical response of the PU interlayer. Numerical research by (Jacobs 2017) indicates that its properties highly affect the shear capacity and the contour plot gained through numerical modelling. An interesting solution would be the engineering of a composite interlayer as described by (Frigo 2017) with a softer external interlayer, to adapt to surface imperfections and displacements occurring under axial load and an inner layer that would be stiffer and more resistant. The research and numerical data obtained so far, as well as the creation of physical prototypes prove the potential and feasibility of the system and encourage the next steps of development towards its application in built structures.

### *Acknowledgements*

The authors gratefully acknowledge Kees Baardolf for his technical assistance and remarkable insight in the manufacturing of the prototypes, Prof. Jiyong Lee for his valuable feedback on the design concepts and Katherine Rutecki for her feedback in kiln-casting.

### **References**

- Akerboom, R.: Glass Columns, exploring the potential of free standing glass columns assembled from stacked cast elements. TU Delft (2016)
- Aurik, M.: Structural Aspects of an Arched Glass Masonry Bridge. Delft University of Technology (2017)
- Aurik, M., Snijder, A., Noteboom, C., Nijse, R., Louter, C.: Experimental analysis on the glass-interlayer system in glass masonry arches. *Glass Structures & Engineering* 3(2), 335-353 (2018). doi:10.1007/s40940-018-0068-7
- Barou, L., Bristogianni, T., Oikonomopoulou, F.: Transparent Restoration. TU Delft (2016)
- Bristogianni, T., Oikonomopoulou, F., Justino de Lima, C., Veer, F.A., Nijse, R.: Cast Glass Components out of Recycled Glass: Potential and limitations of upgrading waste to load-bearing structures. In: Belis, J., Louter, C., Bos, F. (eds.) *Challenging Glass 6 International Conference on the Architectural and Structural Applications of Glass*, Delft 2018
- Christensen, R.M.: *Theory of materials failure*. Oxford University Press, UK (2013)
- Dyskin, A.V., Estrin, Y., Pasternak, E., Khor, H.C., Kanel-Below, A.J.: Fracture Resistant Structures Based on Topological Interlocking with Non-planar Contacts. *Advances Engineering Materials* 5(3), 116-119 (2003). doi:10.1002/adem.200390016
- Dyskin, A.V., Pasternak, E., Estrin, Y.: Mortarless structures based on topological interlocking. *Frontiers of Structural and Civil Engineering* 6(2), 188-197 (2012). doi:10.1007/s11709-012-0156-8
- Estrin, Y., Dyskin, A.V., Pasternak, E.: Topological interlocking as a material design concept. *Materials Science and Engineering C*(31), 1189-1194 (2011)
- Eurostat: Waste Statistics in Europe.  
[http://ec.europa.eu/eurostat/statisticsexplained/index.php/Packaging\\_waste\\_statistics](http://ec.europa.eu/eurostat/statisticsexplained/index.php/Packaging_waste_statistics) (2014). Accessed 22 October 2017
- Frigo, G.: Restoration of partially collapsed historic wall using interlocking cast-glass components: the case of san michele castle in cagliari. Politecnico di Milano (2017)

- Goppert, K., Paech, C., Arbos, F., Teixidor, C.: Innovative Glass Joints - The 11 March Memorial in Madrid. In: Louter, C., Bos, F., Veer, F. (eds.) *Challenging Glass: Conference on Architectural and Structural Applications of Glass*, Delft, The Netherlands 2008, pp. 111-118. IOS Press
- Granta Design Limited: CES EduPack 2015. In. Granta Design Limited, Cambridge, (2015)
- Hannah, B.H.: Jaume Plensa: *Crown Fountain as Carnivalesque*. Umi Dissertation Publishing, USA (2009)
- Hiroshi, N.: Residence in Hiroshima. *DETAIL: Translucent and Transparent 2* (2013)
- Jacobs, E.A.M.: Structural consolidation of historic monuments by interlocking cast glass components. Delft University of Technology (2017)
- Korres, M.: *From Pentelicon to the Parthenon: The Ancient Quarries and the Story of a Half-Worked Column Capital of the First Marble Parthenon*. Oxford University Press, UK (2000)
- Kroller-Muller Museum: Roni Horn: Opposites of white. <http://krollermuller.nl/en/roni-horn-opposites-of-white> (2007). 2016
- Oikonomopoulou, F., Bristogianni, T., Barou, L., Jacobs, E.A.M., Frigo, G., Veer, F.A., Nijse, R.: A novel, demountable structural glass system out of dry-assembly, interlocking cast glass components. In: Louter, C., Belis, J., Bos, F. (eds.) *Challenging Glass 6: Conference on Architectural and Structural Applications of Glass*, The Netherlands 2018
- Oikonomopoulou, F., Bristogianni, T., Nijse, R., Veer, F.A.: Innovative structural applications of adhesively bonded solid glass blocks. In: Vitkala, J. (ed.) *Glass Performance Days*, Tampere 2015a, pp. 256-261.
- Oikonomopoulou, F., Bristogianni, T., Veer, F.A., Nijse, R.: The construction of the Crystal Houses façade: challenges and innovations. *Glass Structures & Engineering*, 1-22 (2017). doi:10.1007/s40940-017-0039-4
- Oikonomopoulou, F., Veer, F.A., Nijse, R., Baardolf, K.: A completely transparent, adhesively bonded soda-lime glass block masonry system. *Journal of Facade Design and Engineering* 2(3-4), 201-222 (2015b). doi:10.3233/fde-150021
- Schober, H., Schneider, J., Justiz, S., Gugeler, J., Paech, C., Balz, M.: Innovations with glass, steel and cables. In: *Glass Performance Days*, Tampere, Finland 2007, pp. 198-201
- Snijder, A., Smits, J., Bristogianni, T., Nijse, R.: Design and Engineering of a Dry Assembled Glass Block Pedestrian Bridge. In: Belis, J., Louter, C., Bos, F. (eds.) *Challenging Glass 5*, Ghent, Belgium 2016. Ghent University

